OAK RIDGE NATIONAL LABORATORY
operated by
UNION CARBIDE CORPORATION
NUCLEAR DIVISION
for the
U.S. ATOMIC ENERGY COMMISSION

ORNL-TM-1994

CREEP-RUPTURE PROPERTIES OF UNALLOYED TANTALUM, Ta-10% W AND T-111 ALLOYS

R. L. Stephenson

NOTICE This document contains information of a preliminary nature and was prepared primarily for internal use at the Oak Ridge National Laboratory. It is subject to revision or correction and therefore does not represent a final report.

ORNL-TM-1994

Contract No. W-7405-eng-26

METALS AND CERAMICS DIVISION

CREEP-RUPTURE PROPERTIES OF UNALLOYED TANTALUM, Ta–10% W AND T-111 ALLOYS

R. L. Stephenson

DECEMBER 1967

OAK RIDGE NATIONAL LABORATORY
Oak Ridge, Tennessee
operated by
UNION CARBIDE CORPORATION
for the
U.S. ATOMIC ENERGY COMMISSION

CONTENTS

CREEP-RUPTURE PROPERTIES OF UNALLOYED TANTALUM, Ta–10% W AND T-111 ALLOYS

R. L. Stephenson

ABSTRACT

The long-time, high-temperature creep properties of unalloyed tantalum, Ta–10% W, and T-111 (Ta–8% W–2% Hf) were studied at 1204, 1427, and 1649°C (2200, 2600, and 3000°F). The Ta–10% W and T-111 were much stronger than unalloyed tantalum. The properties of Ta–10% W and T-111 were almost equal for the thermomechanical histories studied. The ductilities of all three materials were excellent.

INTRODUCTION

In recent years, increasing consideration has been given to tantalum-base alloys for high-temperature structural applications. On the basis of short-time data, the addition of 10% W appears to improve substantially the strength of tantalum.[1] This alloy also appears to have a low ductile-to-brittle transition temperature, improved oxidation resistance, good workability, and good weldability.[1,2]

More recently, hafnium has been added to the binary alloy. This has resulted in the T-111 alloy (Ta–8% W–2% Hf) which also appears to have desirable ductility, weldability, and workability.[2-4] In view of the potential strength offered by Ta–10% W and T-111 it was considered desirable to undertake a systematic study of their long-time (1000 hr) high-temperature creep properties. The creep properties of pure tantalum were also determined, primarily for comparative purposes.

---

[1]M. L. Torti, "90 Ta–10 W Offers High Temperature Strength Plus Ductility," Space/Aeronautics 36, 87–93 (September 1961).

[2]G. G. Lessmann and D. R. Stoner, "Welding Refractory Metal for Space Power System Applications," paper presented at the 9th National SAMPLE Symposium on Joining of Materials for Aerospace Systems Nov. 15–17, 1965, Dayton, Ohio.

[3]R. G. Donnelly and G. M. Slaughter, "Weldability Evaluation of Advanced Refractory Alloys," Welding J. (N.Y.) 45, 250-s–257-s (June 1966).

[4]R. L. Ammon and R. T. Begley, Pilot Production and Evaluations of Tantalum Alloy Sheet, WANL-PR-M-004 (June 1963).

MATERIALS

All materials used in this study were produced by National Research Corporation. Their compositions are shown in Tables 1, 2, and 3. All materials were tested in the cold worked condition.

Table 1. Vendor's Analysis of Unalloyed Tantalum, Heat 2202

Element	Weight Percent
Tungsten	0.004
Molybdenum	0.001
Titanium	0.0005
Copper	0.0001
Aluminum	0.0025
Niobium	0.0032
Silicon	0.0016
Nickel	0.0005
Chromium	< 0.0005
Iron	0.0010
Nitrogen	0.0020
Oxygen	0.0046
Carbon	0.0025
Tantalum	Balance

Table 2. Vendor's Analysis of Ta–10% W, Heat 1862

Element	Weight Percent
Tungsten	9.1
Molybdenum	< 0.0010
Nickel	< 0.0005
Chromium	< 0.0005
Iron	0.0010
Nickel	0.0023
Oxygen	0.0036
Carbon	0.0035
Tantalum	Balance

Table 3. Analyses of T-111 Alloy, Heat 2650

Element	Vendor's Analysis (wt %)	ORNL Analysis (wt %)
Tungsten	7.4	7.5
Hafnium	2.1	1.9
Carbon	0.0049	0.0070
Oxygen	0.0057	0.0053
Hydrogen		0.0004
Nitrogen	0.0023	0.0029
Tantalum	Balance	Balance

EXPERIMENTAL DETAILS

The apparatus used is described in a previous report.[5] The tests were performed at pressures lower than 2×10^{-7} torr. Every test specimen was analyzed for interstitial impurities. The carbon contents of most specimens were less than 100 ppm after testing. The after-test oxygen content of most specimens was between 100 and 300 ppm. It was not possible to detect any systematic dependence of the mechanical properties on the posttest interstitial levels within the ranges mentioned. Sheet specimens 0.60 in. thick with a gage section 3×0.2 in. were used.

The metallographic specimens were prepared by vibratory polishing in a manner described by Long and Gray.[6]

RESULTS AND DISCUSSION

The creep-rupture properties of unalloyed tantalum at 1204°C (2200°F) are given in Fig. 1. Times to 1, 2, 5, and 10% creep are plotted as a function of stress along with the time to rupture. Similarly, the creep-rupture properties at 1427°C (2600°F) and 1649°C (3000°F) are given in

[5]R. L. Stephenson, Comparative Creep-Rupture Properties of D-43 and B-66 Alloys, ORNL-TM-944 (November 1964).

[6]E. L. Long, Jr., and R. J. Gray, Metals Progr. 74(4), 145–148 (October 1958).

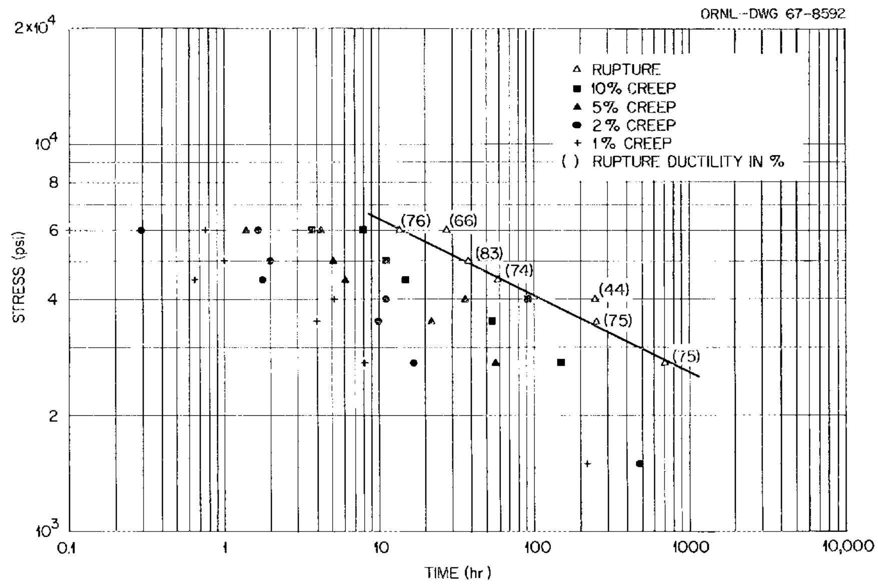

Fig. 1. Creep-Rupture Properties of Unalloyed Tantalum at 1204°C (2200°F).

Figs. 2 and 3, respectively. Figure 4 gives the secondary creep rate as a function of stress for these three temperatures.

The creep-rupture properties of Ta–10% W alloy at 1204°C (2200°F) are shown in Fig. 5. Times to 1, 2, 5, and 10% creep are shown as a function of stress along with the time to rupture. Similarly, the creep-rupture

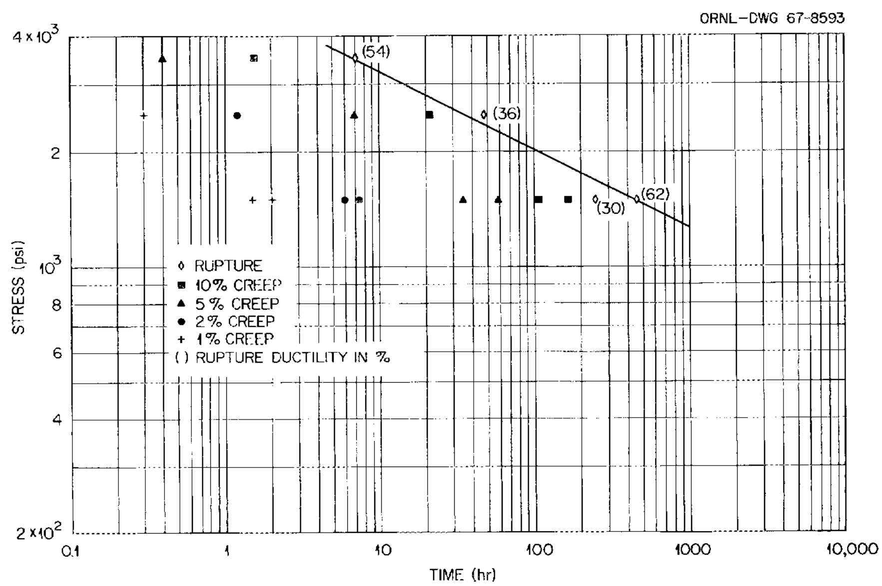

Fig. 2. Creep-Rupture Properties of Unalloyed Tantalum at 1427°C (2600°F).

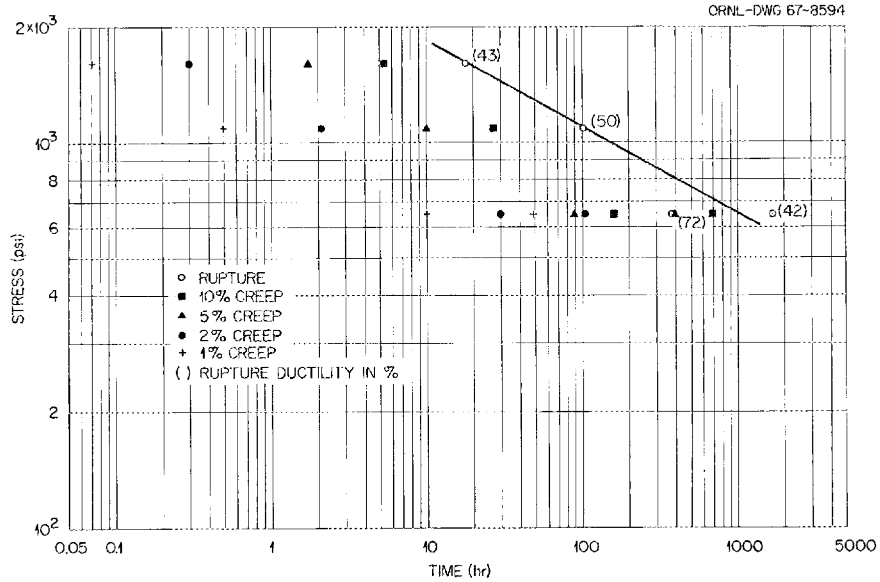

Fig. 3. Creep-Rupture Properties of Unalloyed Tantalum at 1649°C (3000°F).

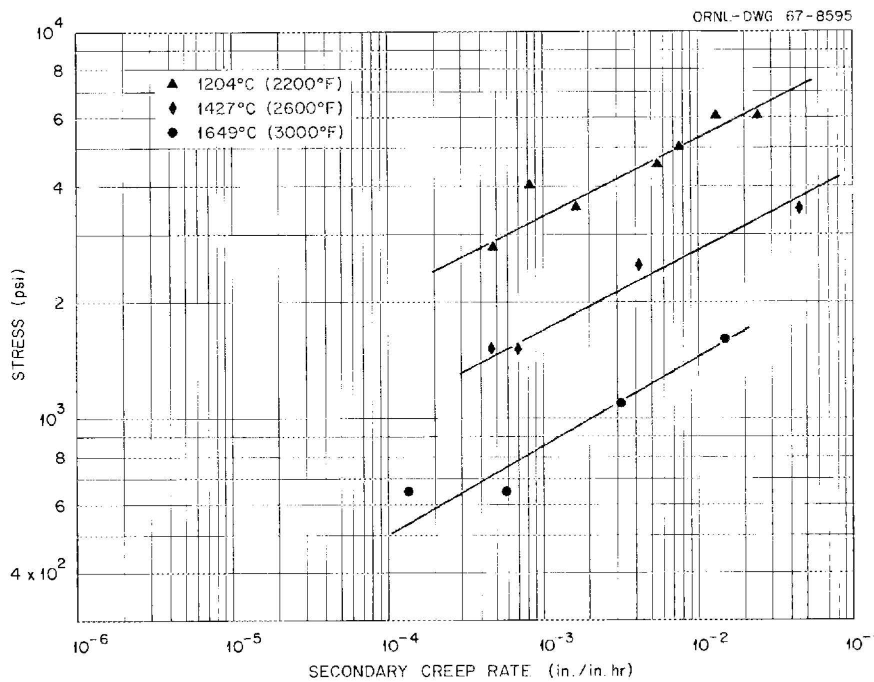

Fig. 4. Secondary Creep Rate vs Stress for Unalloyed Tantalum.

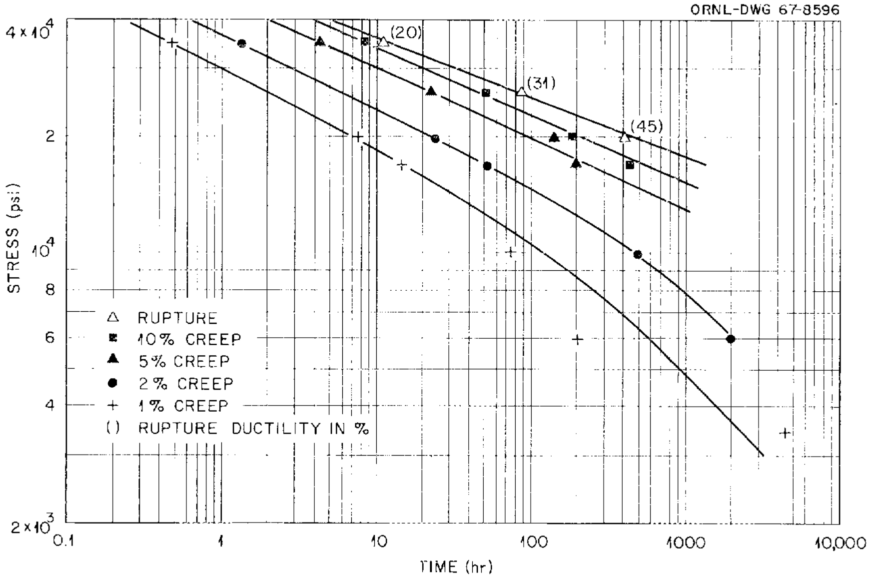

Fig. 5. Creep-Rupture Properties of Ta–10% W Alloy at 1204°C (2200°F).

properties at 1427°C (2600°F) and 1649°C (3000°F) are given in Figs. 6 and 7, respectively. The secondary creep rate is given as a function of stress for these three temperatures in Fig. 8.

Figure 9 gives the creep-rupture properties of T-111 at 1204°C (2200°F). Similar curves are given for T-111 at 1427°C (2600°F) and

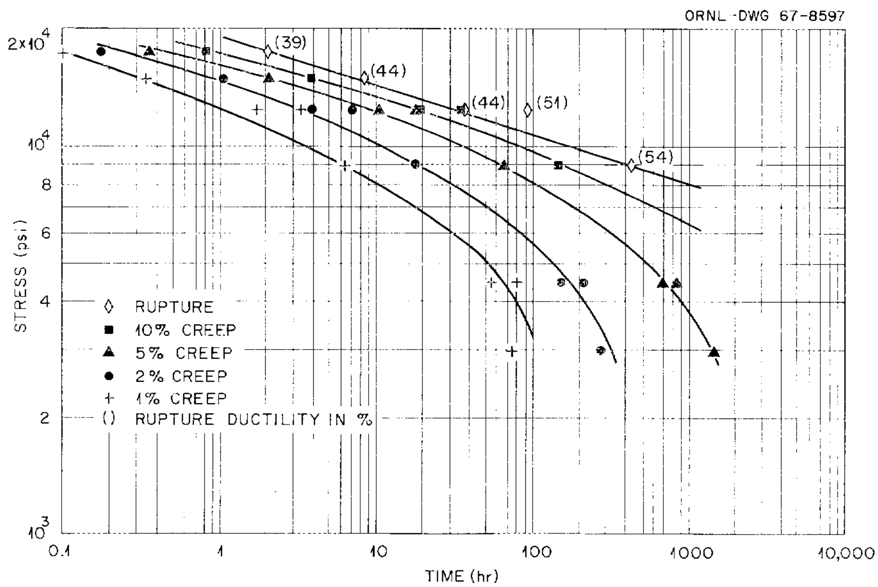

Fig. 6. Creep-Rupture Properties of Ta–10% W Alloy at 1427°C (2600°F).

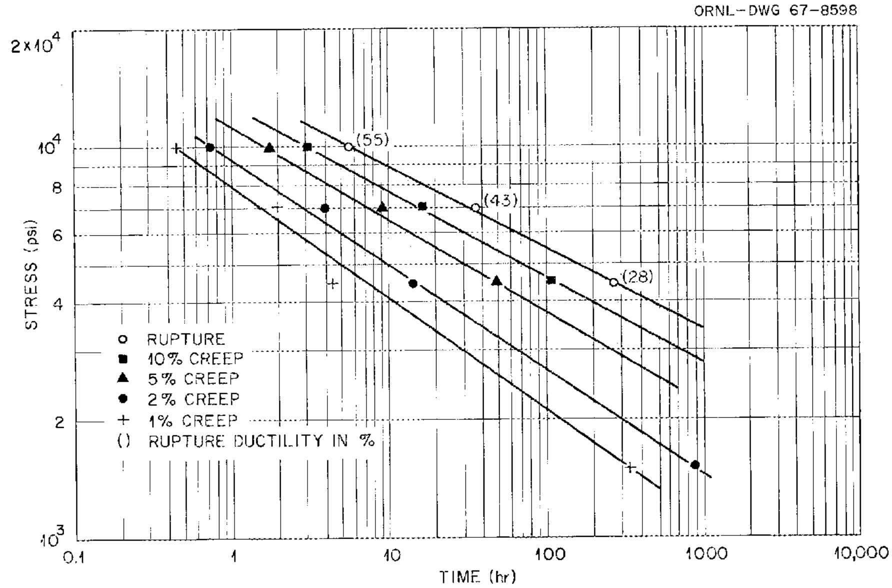

Fig. 7. Creep-Rupture Properties of Ta–10% W Alloy at 1649°C (3000°F).

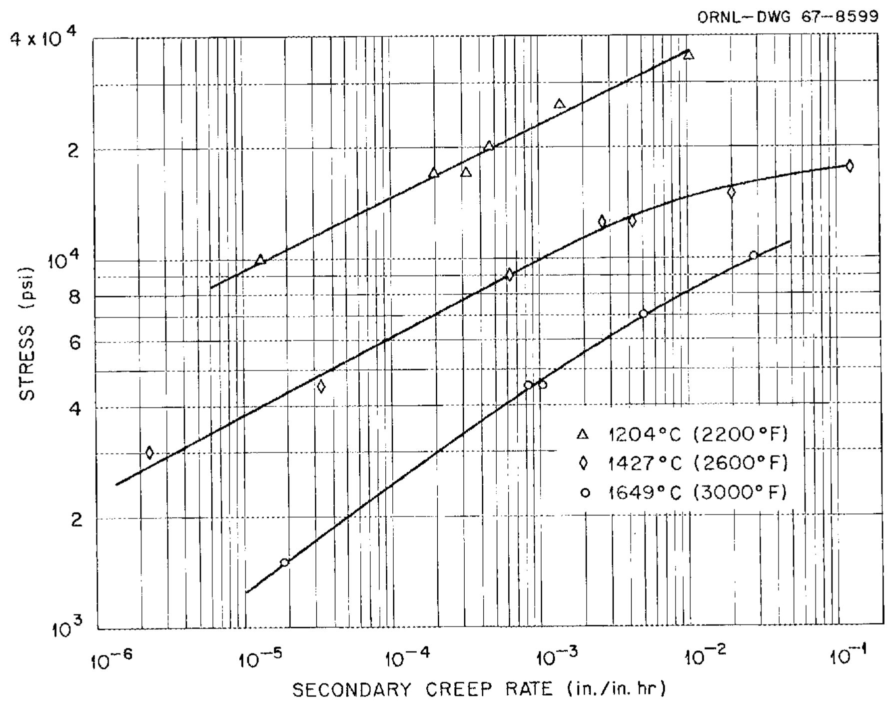

Fig. 8. Secondary Creep Rate vs Stress for Ta–10% W Alloy.

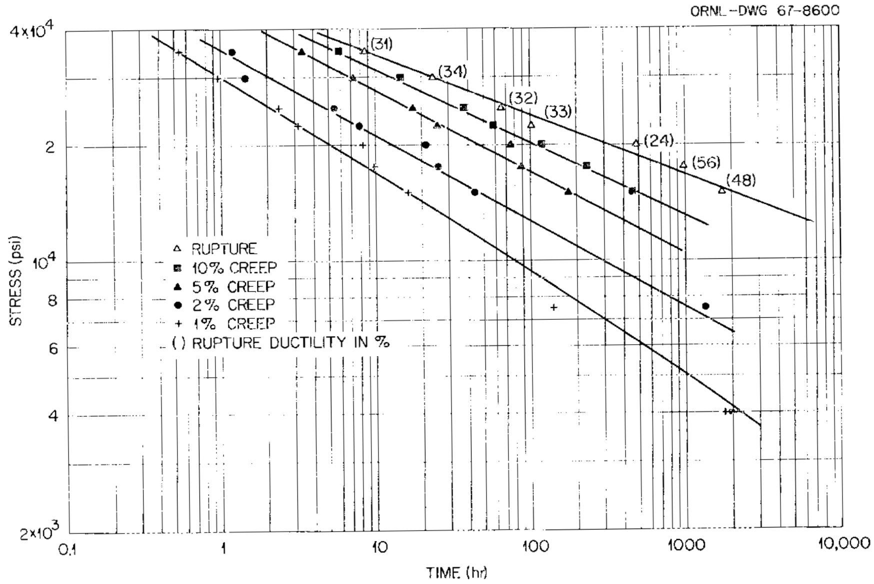

Fig. 9. Creep-Rupture Properties of T-111 Alloy at 1204°C (2200°F).

1649°C (3000°F) in Figs. 10 and 11, respectively. Figure 12 gives the secondary creep rate as a function of stress at these temperatures.

The rupture elongation in percent is given in parentheses beside each point on the stress-rupture curves. In all three materials the ductilities are excellent.

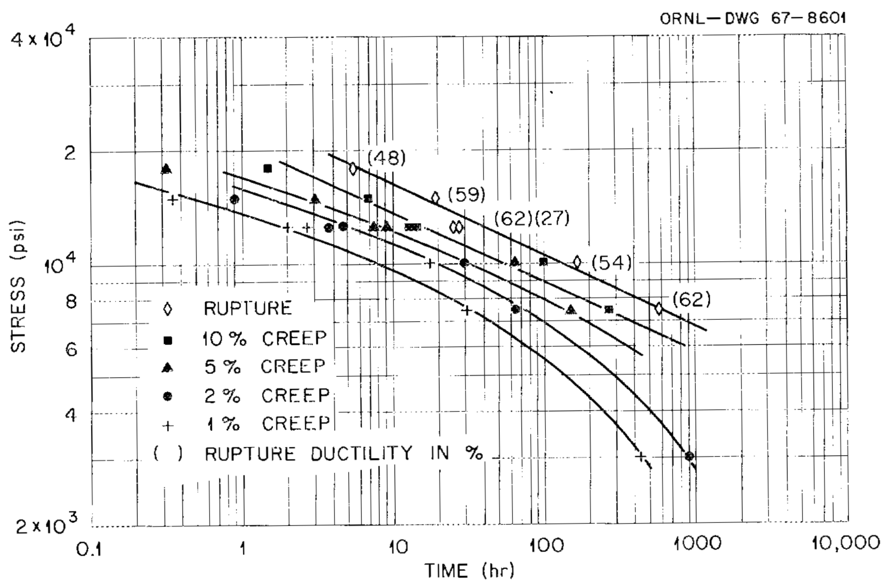

Fig. 10. Creep-Rupture Properties of T-111 Alloy at 1427°C (2600°F).

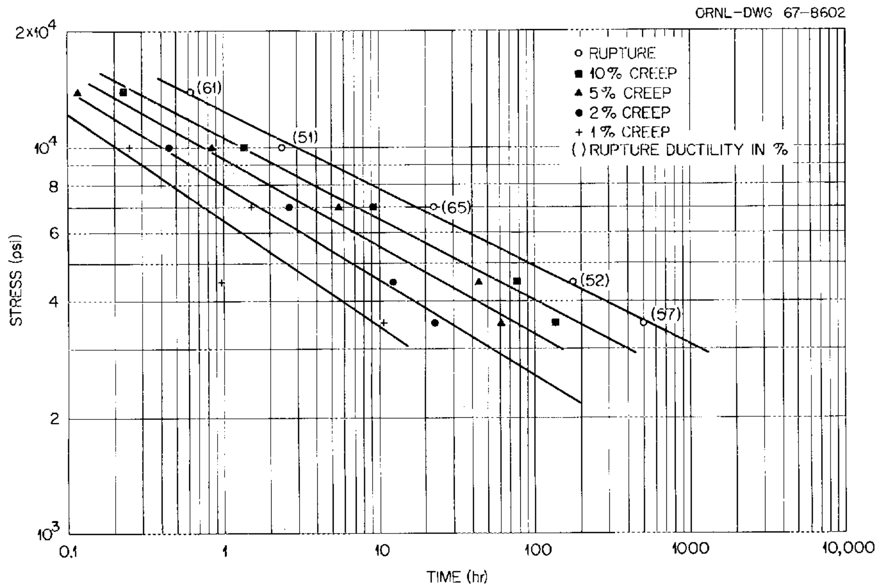

Fig. 11. Creep-Rupture Properties of T-111 Alloy at 1649°C (3000°F).

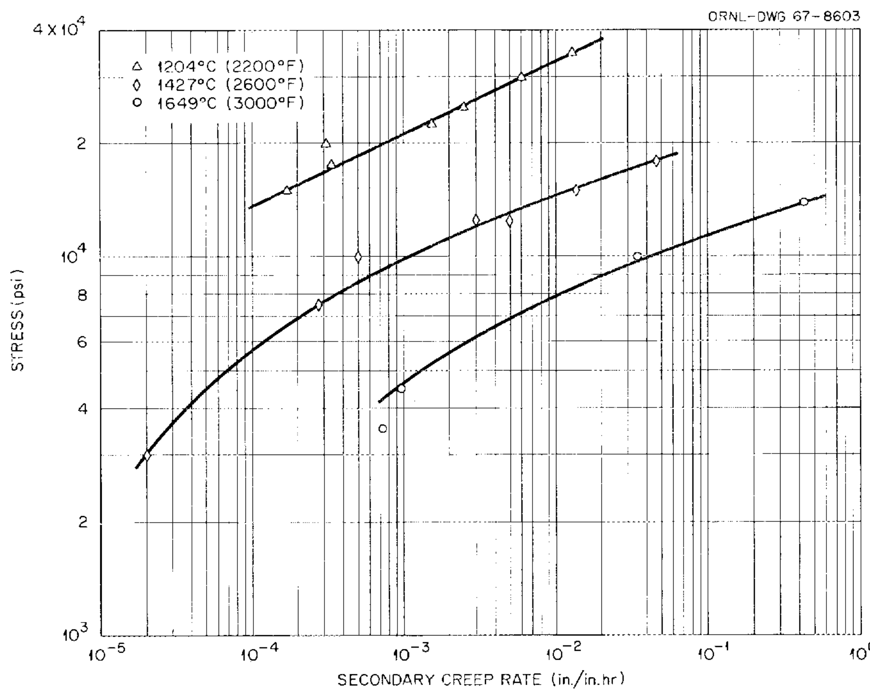

Fig. 12. Secondary Creep Rate vs Stress for T-111 Alloy.

Figure 13 shows a photomicrograph of an unalloyed tantalum specimen with a rupture life of 27.5 hr at 1204°C (2200°F). It is clear that the material has recrystallized and attained a substantial grain size under these conditions. Specimens tested for longer times at correspondingly lower stresses frequently develop a pronounced substructure rather than a larger grain size. Figure 14 shows a microstructure typical of these specimens.

At 1427°C (2600°F), only a short time is required for the development of quite large grains in unalloyed tantalum. This is illustrated by the photomicrograph of a specimen with a rupture life of 7.0 hr at this temperature, shown in Fig. 15. Figure 16 shows the microstructure of a specimen tested at a stress which produced failure in 466.0 hr at 1427°C (2600°F). The microstructure is similar in appearance to the subgrains in Fig. 14, except that these small areas give the appearance of being

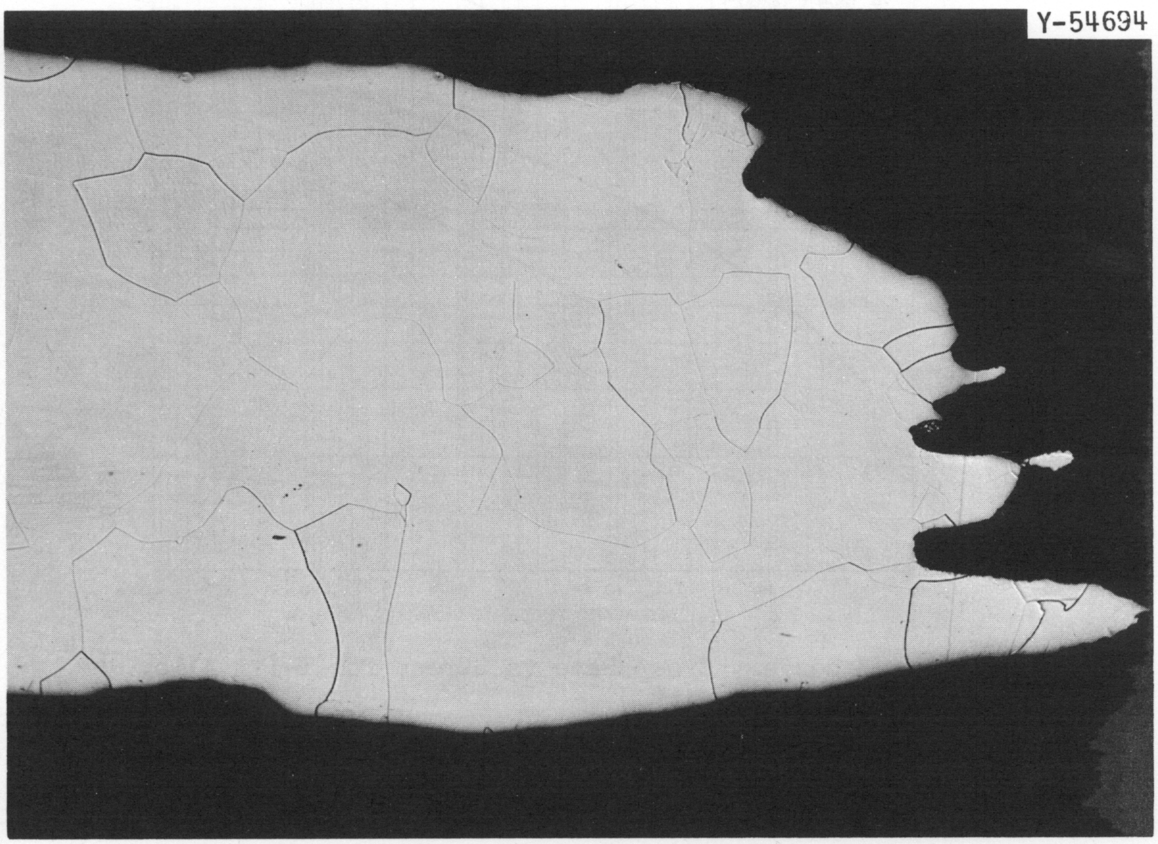

Fig. 13. Photomicrograph of Unalloyed Tantalum Specimen Which Failed After 27.5 hr at 6000 psi and 1204°C (2200°F). Etchant: NH_4–H_2O–HF. 100×.

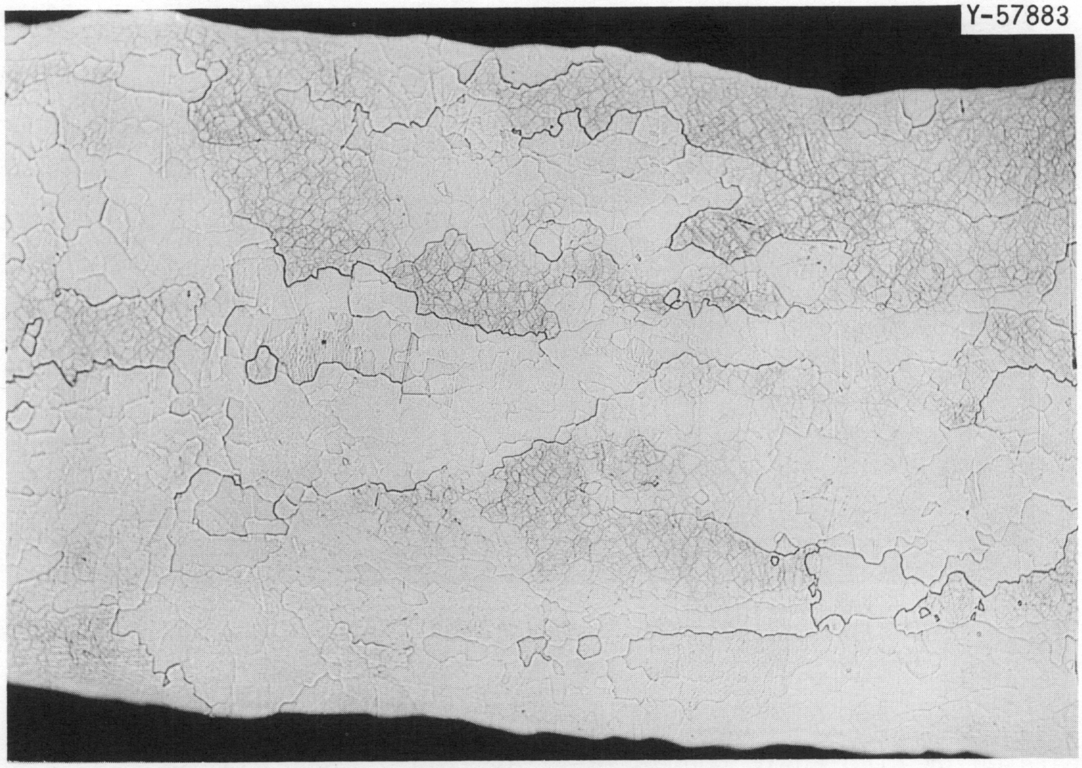

Fig. 14. Photomicrograph of Unalloyed Tantalum Specimen Which Failed After 693.6 hr at 2750 psi and 1204°C (2200°F). 100×. Reduced 6%.

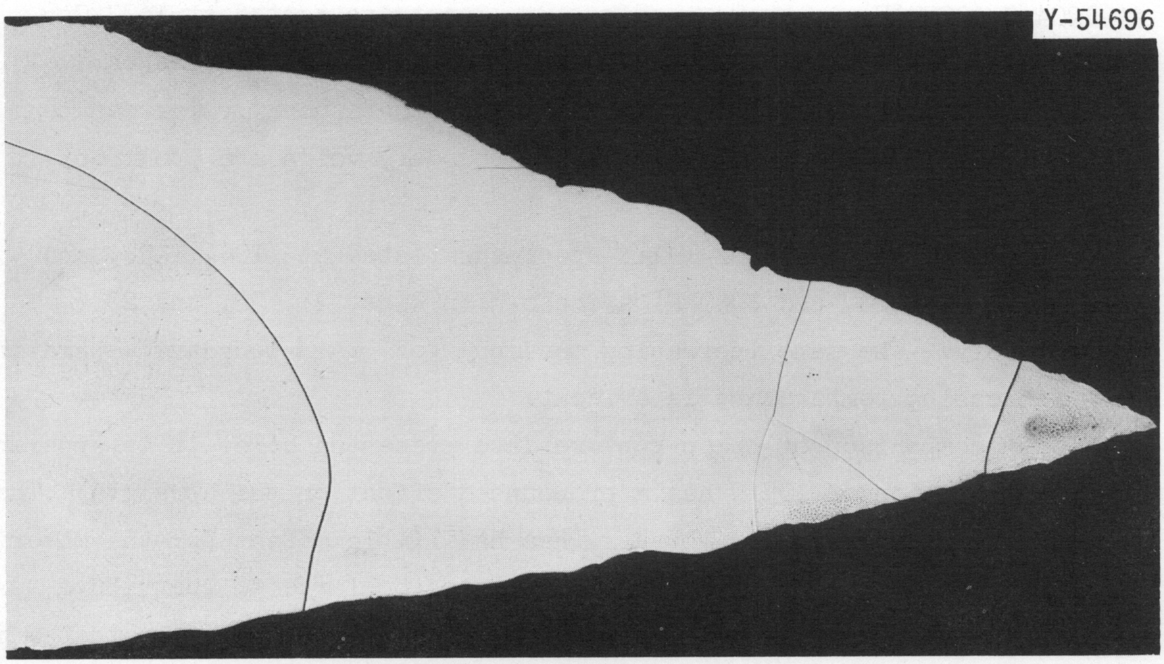

Fig. 15. Photomicrograph of Unalloyed Tantalum Specimen Which Failed After 7.0 hr at 3500 psi and 1427°C (2600°F). 100×.

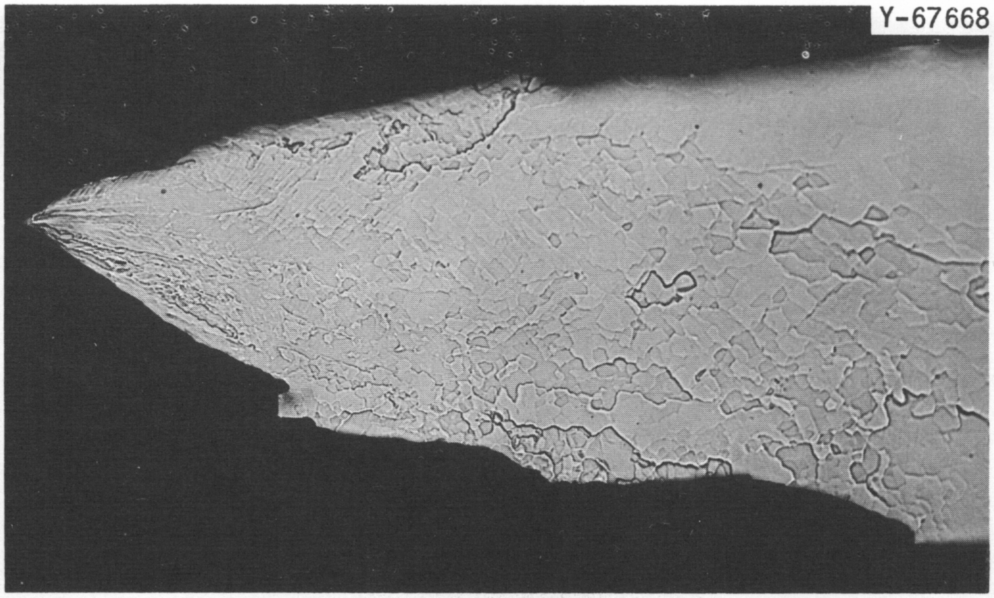

Fig. 16. Photomicrograph of Unalloyed Tantalum Specimen Which Failed After 466.0 hr at 1500 psi and 1427°C (2600°F). 100×.

separated by high angle boundaries. At 1649°C (3000°F), very large grains are developed, as shown in Fig. 17. It is noteworthy that in no case are voids observed.

The microstructure of a Ta–10% W specimen which failed after 737.3 hr at 1204°C (2200°F) is shown in Fig. 18. Specimens tested at 1427°C (2600°F) and 1649°C (3000°F) are shown in Figs. 19 and 20, respectively. A slight tendency toward the formation of grain-boundary voids can be seen in Fig. 19, while very large grain-boundary voids are prominent in Fig. 20.

The microstructures of T-111 specimens tested at 1204, 1427, and 1649°C (2200, 2600, and 3000°F) are shown in Figs. 21, 22, and 23, respectively. The same increasing tendency for grain-boundary separation with increasing temperature is evident.

Upon comparison of creep-rupture data presented here, it is apparent that the addition of 10% W has a pronounced effect on the strength. The further addition of 2% Hf, however, has had little effect for the material histories examined here. Since precipitates too large to contribute to dispersion strengthening are observed (Fig. 23), it is possible that a heat treatment which places these in solution and reprecipitates them in a more finely dispersed state may produce an improvement of T-111 over Ta–10% W.

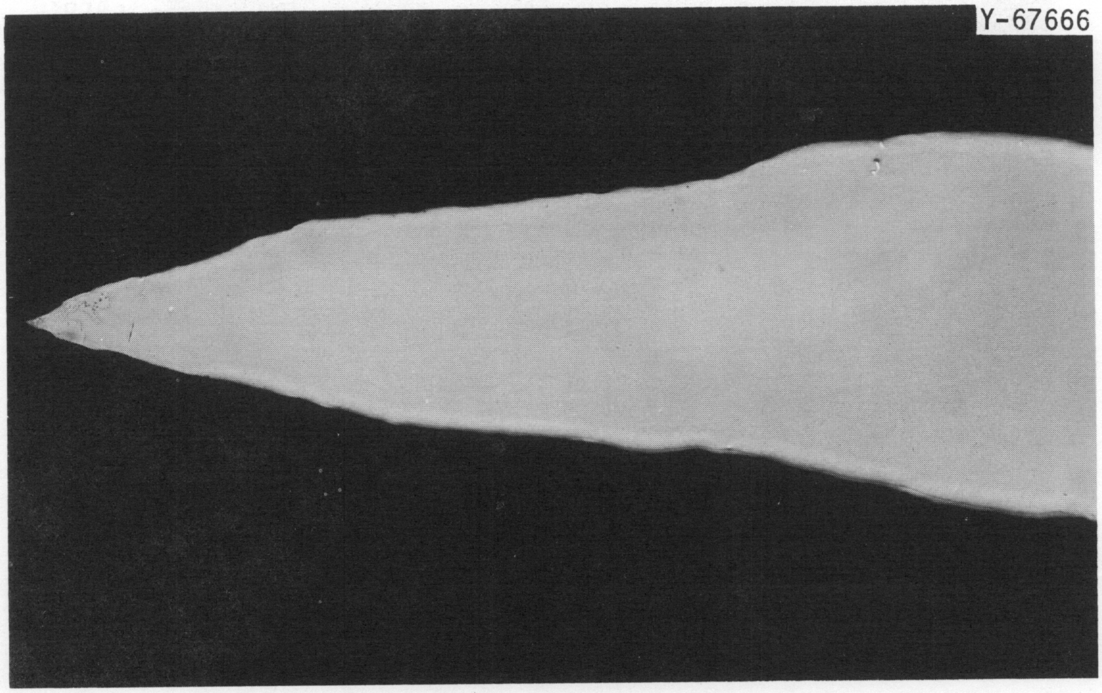

Fig. 17. Photomicrograph of Unalloyed Tantalum Specimen Which Failed After 374.9 hr at 650 psi and 1649°C (3000°F). 100×.

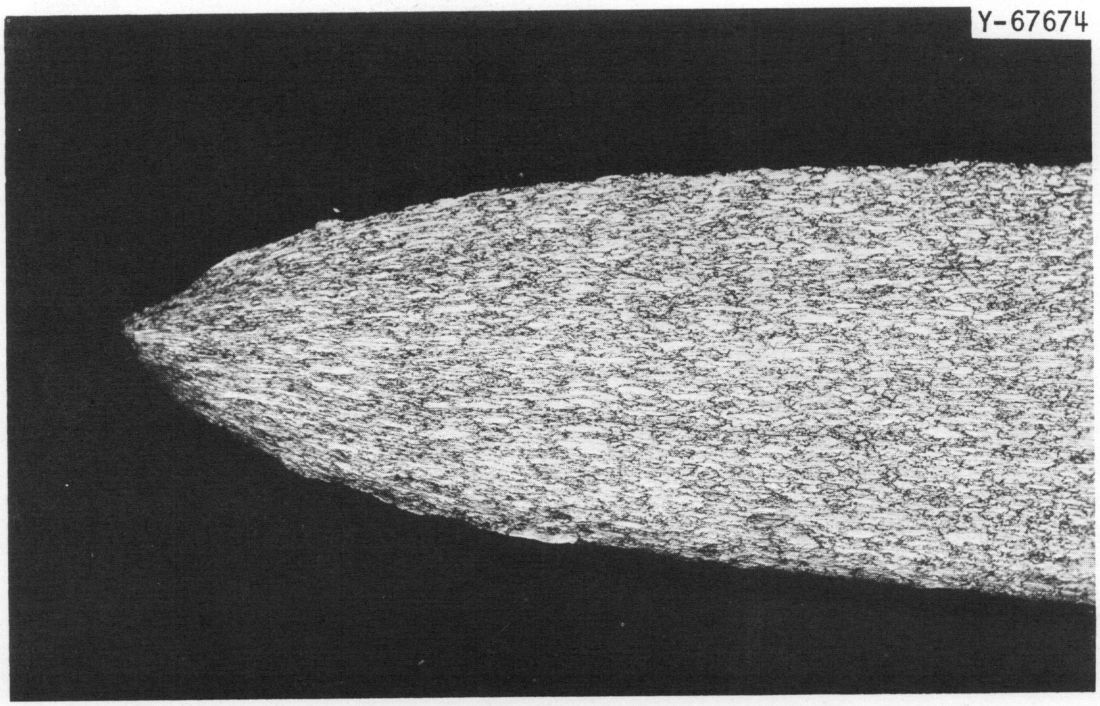

Fig. 18. Photomicrograph of Ta—10% W Specimen Which Failed After 737.3 hr at 17,000 psi and 1204°C (2200°F). Etchant: 25 HF—25 HNO_3—5 glycerin. 100×.

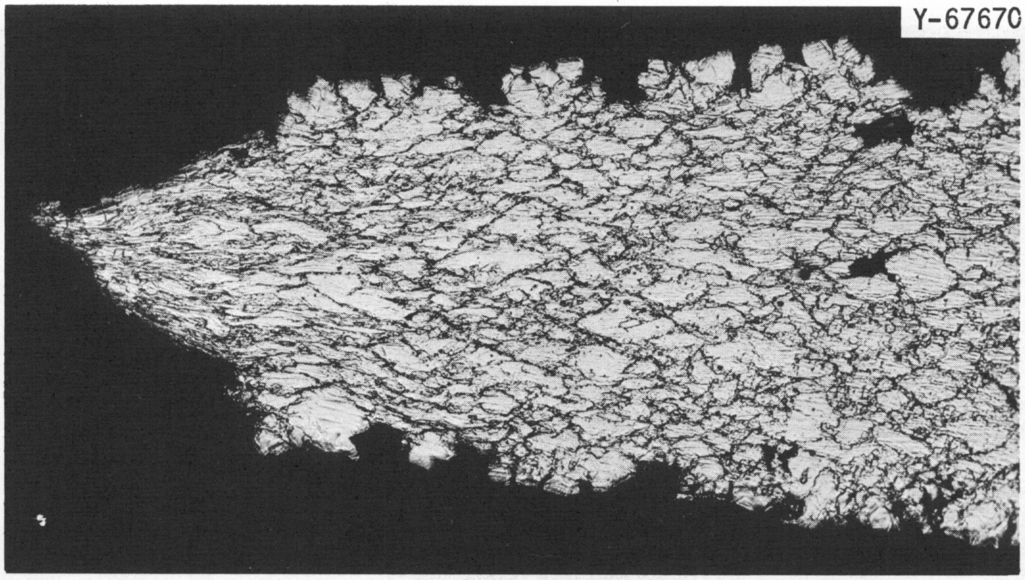

Fig. 19. Photomicrograph of Ta–10% W Specimen Which Failed After 441.8 hr at 9000 psi and 1427°C (2600°F). 100×.

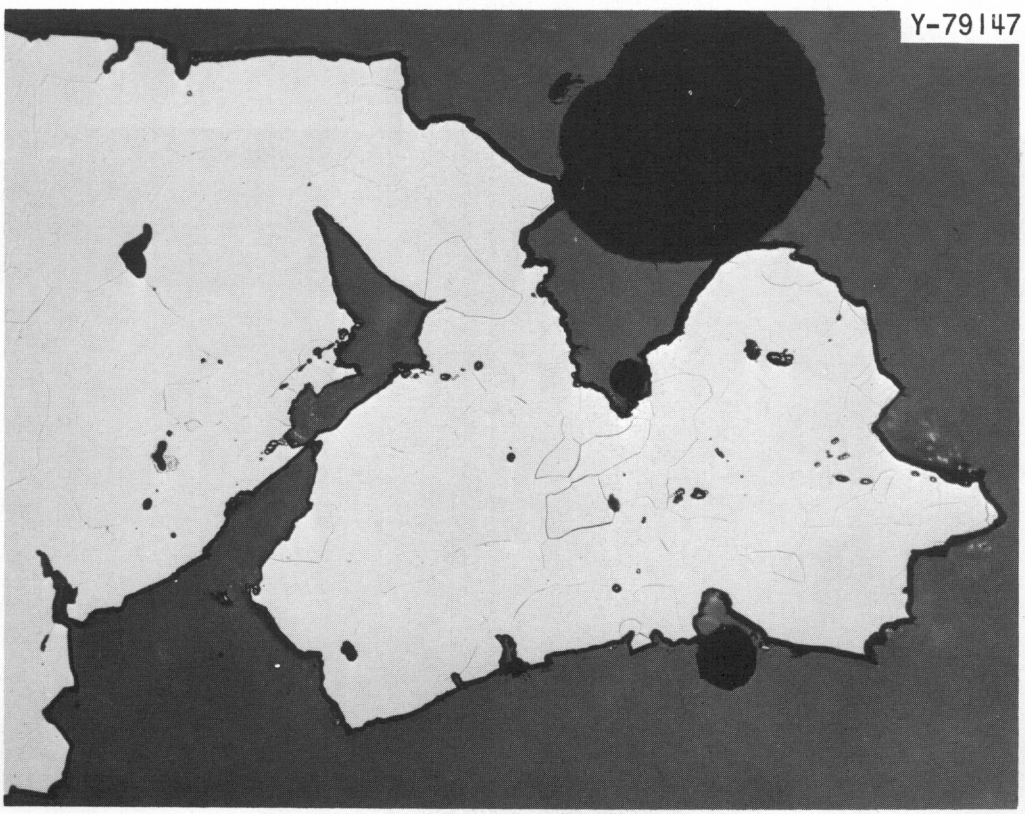

Fig. 20. Photomicrograph of Ta–10% W Specimen Which Failed After 270.6 hr at 4500 psi and 1649°C (3000°F). 100×.

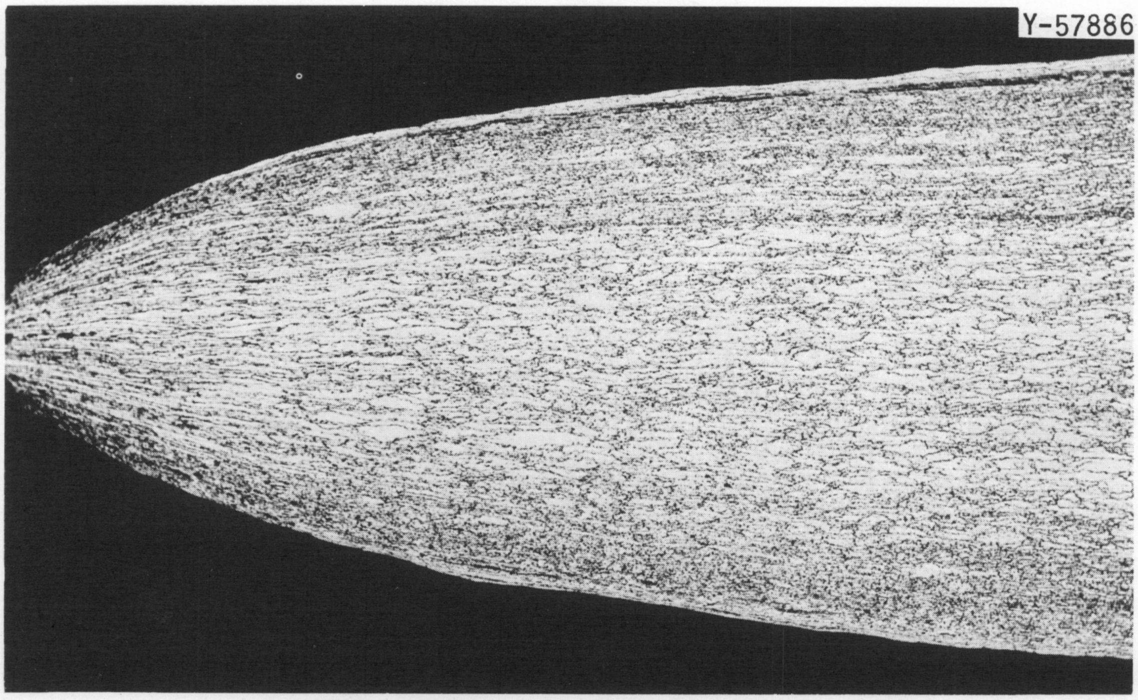

Fig. 21. Photomicrograph of T-111 Alloy Specimen Which Failed After 975.1 hr at 17,500 psi and 1204°C (2200°F). Etchant: H_2O–HF–NHO_3–H_2SO_4. 100×.

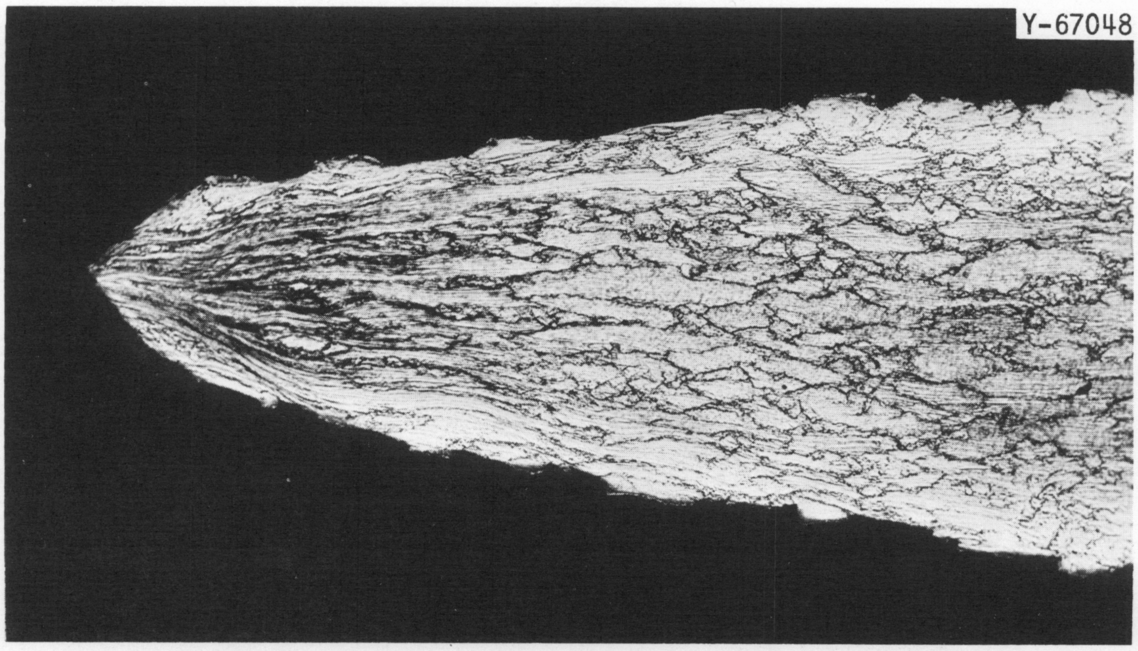

Fig. 22. Photomicrograph of T-111 Alloy Specimen Which Failed After 575.4 hr at 7500 psi and 1427°C (2600°F). 100×.

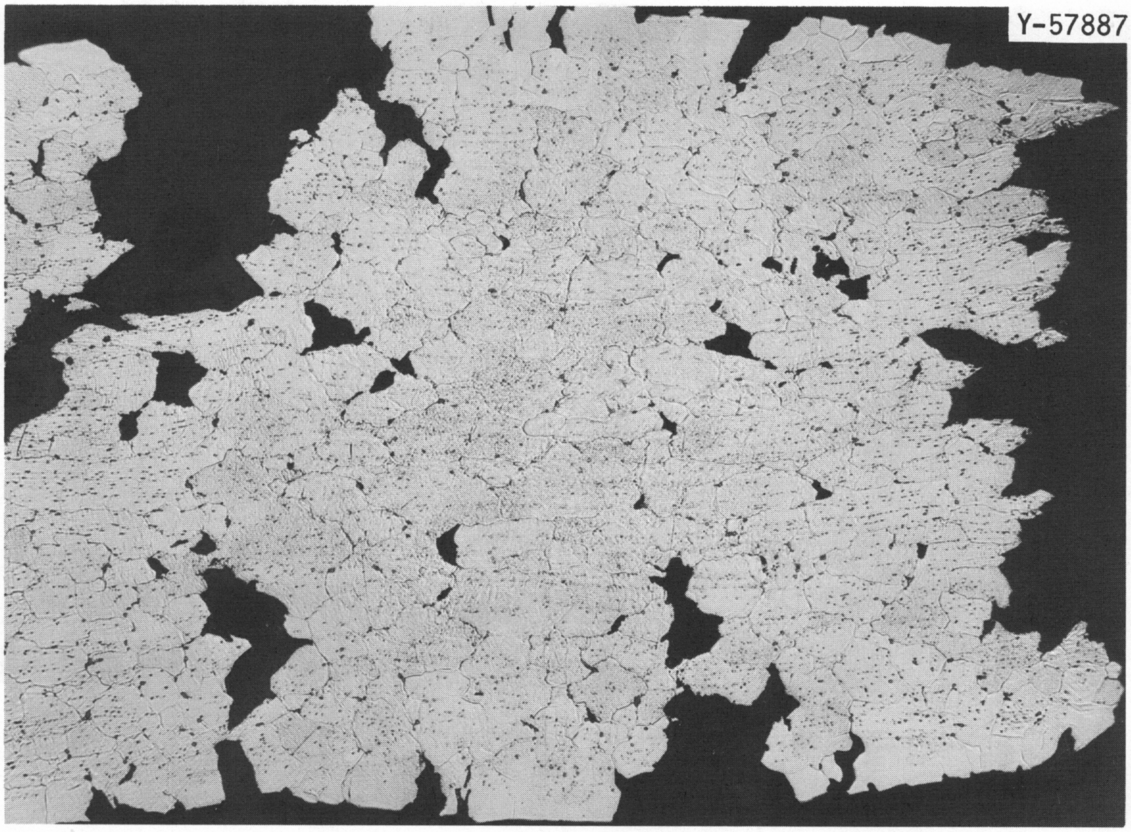

Fig. 23. Photomicrograph of T-111 Alloy Specimen Which Failed After 493.2 hr at 3500 psi and 1649°C (3000°F). 100×.

The microstructures of the unalloyed tantalum appear very clean; those of the Ta–10% alloy show only a slight indication of a precipitate while precipitates are distinctly visible in the T-111 alloy microstructures. Grain growth is much faster in tantalum than in Ta–10% W or T-111. Grain growth appears to be slightly greater in Ta–10% W than in T-111 at 1427 and 1649°C (2600 and 3000°F). The precipitates in T-111 are probably HfC and HfO_2 and may be responsible for the additional grain-growth inhibition.

SUMMARY AND CONCLUSIONS

The creep-rupture properties of cold worked tantalum, Ta–10% W, and T-111 (Ta–8% W–2% Hf) at 1204, 1427, and 1649°C (2200, 2600, and 3000°F) are presented. It is apparent from these data that substantial solution strengthening is derived from the addition of tungsten to tantalum. No further strengthening was observed upon the addition of hafnium to this binary alloy for the material conditions investigated. However, some additional grain-size stabilization was noted in the T-111, possibly due to hafnium-base precipitates in the microstructure.

Good rupture ductilities were observed in all cases.

ACKNOWLEDGMENTS

The author wishes to express his appreciation for the contribution made to this work by others. Those who merit specific mention J. R. Weir, Jr. for guidance and suggestions during the course of the work, H. R. Gaddis and C. W. Houck for the preparation of the photomicrographs, C. K. Thomas for performance of the experimental details, H. Inouye and H. E. McCoy, Jr. for review of the manuscript, and the Metals and Ceramics Division Reports Office for the preparation of this report.

INTERNAL DISTRIBUTION

1–3. Central Research Library
4–5. ORNL – Y-12 Technical Library
Document Reference Section
6–15. Laboratory Records
16. Laboratory Records, ORNL R.C.
17. ORNL Patent Office
18. G. M. Adamson, Jr.
19. S. E. Beall
20. D. T. Bourgette
21. G. E. Boyd
22. E. J. Breeding
23. D. A. Canonico
24. K. V. Cook
25. F. L. Culler
26. C. A. Cunningham
27. J. E. Cunningham
28. J. H. DeVan
29. J. H. DiStefano
30–44. R. G. Donnelly
45. W. S. Ernst
46. J. I. Federer
47. A. P. Fraas
48. J. H Frye, Jr.
49. L. C. Fuller
50. J. M. Googin (Y-12)
51. J. L. Gregg
52. W. R. Grimes
53. A. G. Grindell
54. W. O. Harms
55–59. M. R. Hill
60. H. W. Hoffman
61. W. R. Huntley
62. H. Inouye
63. D. H. Jansen
64. G. W. Keilholtz
65. A. P. Litman
66. R. N. Lyon
67. H. G. MacPherson
68. R. E. MacPherson
69. R. W. McClung
70. H. E. McCoy
71. R. E. McDonald
72. D. L. McElroy
73. F. R. McQuilkin
74. A. J. Miller
75. R. E. Moore
76. M. F. Osborne
77. P. Patriarca
78. G. A. Reimann
79. W. C. Robinson, Jr.
80. A. W. Savolainen
81. J. E. Savolainen
82. J. L. Scott
83. A. C. Schaffhauser
84. C. E. Sessions
85. G. M. Slaughter
86. S. H. Smiley (K-25)
87–101. R. L. Stephenson
102. J. E. Strain
103. D. A. Sundberg
104. R. W. Swindeman
105. S. C. Weaver
106. A. M. Weinberg
107. J. R. Weir, Jr.
108. H. C. Young
109. J. Zasler

EXTERNAL DISTRIBUTION

110. C. H. Armbruster, Wright-Patterson AFB
111–113. V. P. Calkins, General Electric, NMPO
114. S. S. Christopher, Combustion Engineering, Windsor, Connecticut
115. D. F. Cope, RDT, SSR, AEC, Oak Ridge National Laboratory
116. J.W.R. Creagh, NASA, Lewis Research Center
117. J. Davis, Jet Propulsion Laboratory
118. R. W. Dayton, Battelle Memorial Institute
119. D. DeHalas, Pacific Northwest Laboratory, Richland, Washington
120. G. K. Dicker, AEC, Washington
121. J. K. Elbaum, Code MAMP, Wright-Patterson AFB

122. D. C. Goldberg, Westinghouse Astronuclear Laboratory
123–124. D. H. Gurinsky, Brookhaven National Laboratory
125. R. Hall, NASA, Lewis Research Center
126. R. C. Hamilton, Institute for Defense Analyses, 1666 Connecticut Ave., N.W., Washington, D.C.
127. Willis Harbaugh, RCA Corp., Lancaster, Pa.
128. E. E. Hoffman, General Electric, Cincinnati
129. J. Jacobs, Sandia Corporation, Sandia Base, Albuquerque, New Mexico
130. J. S. Kane, University of California, LRL
131. H. Kato, U.S. Department of the Interior, Bureau of Mines, Albany, Oregon
132. W. J. Larkin, AEC, Oak Ridge Operations
133. P. J. Levine, Westinghouse Advanced Reactor Division, Waltz Mill Site, Madison, Pa.
134. J. J. Lynch, NASA, Washington, D.C.
135. R. Mayfield, ANL
136. J. McGurty, General Electric, NMPO
137. T. P. Moffitt, NASA, Lewis Research Center
138. T. A. Moss, NASA, Lewis Research Center
139. R. A. Noland, Argonne National Laboratory
140. Louis Rosenblum, NASA, Lewis Research Center
141. W. E. Ray, Westinghouse Advanced Reactor Division, Waltz Mill Site, Madison, Pa.
142. B. Rubin, University of California, LRL
143. N. D. Sanders, NASA, Lewis Research Center
144. H. Schwartz, NASA, Lewis Research Center
145. F. C. Schwenk, AEC, Washington
146–150. J. M. Simmons, AEC, Washington
151. E. E. Stansbury, University of Tennessee
152. D. K. Stevens, AEC, Washington
153. A. Van Echo, AEC, Washington
154. G. W. Wensch, AEC, Washington
155. Glenn Whiting, Sandia Corp., Albuquerque, New Mexico
156. G. A. Whitlow, Westinghouse Advanced Reactor Division, Waltz Mill Site, Madison, Pa.
157. Laboratory and University Division, AEC, ORO
158–172. Division of Technical Information Extension